



**HAL**  
open science

# THERMALLY INDUCED TRANSFORMATION OF MAGNETIC MINERALS IN SOIL BASED ON ROCK MAGNETIC STUDY AND MÖSSBAUER ANALYSIS

M. Jeleńska, A. Hasso-Agopsowicz, B. Kopcewicz

► **To cite this version:**

M. Jeleńska, A. Hasso-Agopsowicz, B. Kopcewicz. THERMALLY INDUCED TRANSFORMATION OF MAGNETIC MINERALS IN SOIL BASED ON ROCK MAGNETIC STUDY AND MÖSSBAUER ANALYSIS. *Physics of the Earth and Planetary Interiors*, 2010, 179 (3-4), pp.164. 10.1016/j.pepi.2009.11.004 . hal-00624828

**HAL Id: hal-00624828**

**<https://hal.science/hal-00624828>**

Submitted on 20 Sep 2011

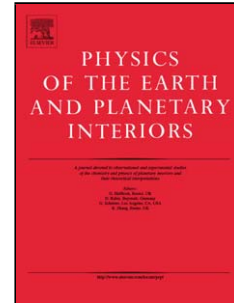
**HAL** is a multi-disciplinary open access archive for the deposit and dissemination of scientific research documents, whether they are published or not. The documents may come from teaching and research institutions in France or abroad, or from public or private research centers.

L'archive ouverte pluridisciplinaire **HAL**, est destinée au dépôt et à la diffusion de documents scientifiques de niveau recherche, publiés ou non, émanant des établissements d'enseignement et de recherche français ou étrangers, des laboratoires publics ou privés.

## Accepted Manuscript

Title: THERMALLY INDUCED TRANSFORMATION OF  
MAGNETIC MINERALS IN SOIL BASED ON ROCK  
MAGNETIC STUDY AND MÖSSBAUER ANALYSIS

Authors: M. Jeleńska, A. Hasso-Agopsowicz, B. Kopcewicz



PII: S0031-9201(09)00237-4  
DOI: doi:10.1016/j.pepi.2009.11.004  
Reference: PEPI 5226

To appear in: *Physics of the Earth and Planetary Interiors*

Received date: 2-12-2008  
Revised date: 21-9-2009  
Accepted date: 20-11-2009

Please cite this article as: Jeleńska, M., Hasso-Agopsowicz, A., Kopcewicz, B., THERMALLY INDUCED TRANSFORMATION OF MAGNETIC MINERALS IN SOIL BASED ON ROCK MAGNETIC STUDY AND MÖSSBAUER ANALYSIS, *Physics of the Earth and Planetary Interiors* (2008), doi:10.1016/j.pepi.2009.11.004

This is a PDF file of an unedited manuscript that has been accepted for publication. As a service to our customers we are providing this early version of the manuscript. The manuscript will undergo copyediting, typesetting, and review of the resulting proof before it is published in its final form. Please note that during the production process errors may be discovered which could affect the content, and all legal disclaimers that apply to the journal pertain.

1 **THERMALLY INDUCED TRANSFORMATION OF MAGNETIC MINERALS IN**  
2 **SOIL BASED ON ROCK MAGNETIC STUDY AND MÖSSBAUER ANALYSIS.**

3

4 M. Jeleńska<sup>1\*</sup>, A. Hasso-Agopsowicz<sup>1</sup>, B. Kopcewicz<sup>1</sup>

5 <sup>1</sup> Institute of Geophysics, Polish Academy of Sciences, Ks. Janusza 64, 01-452 Warsaw,  
6 Poland

7 Maria Jeleńska, Institute of Geophysics, Polish Academy of Sciences, Ks. Janusza 64, 01-452  
8 Warsaw, Poland; phone: +48 22 9615762; fax: +48 22 6915915; e-mail: [bogna@igf.edu.pl](mailto:bogna@igf.edu.pl)

9

10 **ABSTRACT**

11 The purpose of this study is to detect thermal transformations of magnetic minerals occurring  
12 during thermomagnetic susceptibility analysis based on the example of chernozem soil  
13 samples from Ukraine. Rock magnetic methods such as thermal decay of saturation remanent  
14 magnetization (SIRM), hysteresis loops and monitoring of magnetic susceptibility (k) during  
15 heating from temperature of liquid nitrogen (-196°C) up to 700 °C were used as indicators of  
16 magnetic mineralogy, grain size and concentration. In addition, the changes in mineralogy  
17 caused by heating were monitored by Mössbauer analysis. The samples were taken from the  
18 topsoil and from the loess layer of the unpolluted chernozem profile from the Homutovsky  
19 Steppe (East-South Ukraine). SIRM(T) curves and Mössbauer analysis revealed maghemite,  
20 hematite and goethite in the topsoil and in the loess. Low- temperature susceptibility  
21 experiments showed superparamagnetic (SP) - like behaviour in the topsoil and paramagnetic  
22 - like behaviour in the loess. The specimens were heated during susceptibility measurements  
23 in KLY-3 device from room temperature up to subsequent increasing temperatures: 250 °C,  
24 400 °C, 500 °C, 600 °C and 700 °C. After heating to particular temperature, low temperature  
25 experiments, SIRM(T) curves, hysteresis loops and Mössbauer analysis were performed.

26 Additionally, the sample of topsoil and the sample of loess were heated several times to the  
27 increasing temperatures. Mössbauer analysis showed increase of  $\text{Fe}^{2+}$  ions indicating  
28 reduction process during heating. We suggest that in the topsoil, the prevailing  
29 transformations are inversion of hydroxides such as goethite and ferrihydrite to  
30 magnetite/maghemite which occur at temperature 200 – 450 °C, whereas in the loess  
31 reduction of lithogenic hematite to magnetite at temperature above 600°C plays important  
32 role. The topsoil and loess do not differ significantly in such pedogenic parameters as pH,  
33 total iron content  $\text{Fe}_t$  or free iron  $\text{Fe}_d$ . The main differences are in humus and amorphous iron  
34 content  $\text{Fe}_o$ .

35 Keywords: magnetic mineral, thermal transformations, soil, Mössbauer analysis

36

## 37 INTRODUCTION

38 The most prominent feature of ferromagnetic minerals (including ferri- and  
39 antiferromagnetics) is the Curie ( $T_c$ ) or Néel ( $T_N$ ) temperature at which these minerals lose  
40 their properties and become paramagnetics. The Curie and Néel temperatures are widely used  
41 for identification of ferromagnetic minerals. For this purpose temperature dependence of  
42 magnetization acquired in high magnetic field  $M(T)$  or temperature dependence of low-field  
43 volume specific susceptibility  $k(T)$  has been used. In paleomagnetic study, thermal  
44 demagnetization of saturation isothermal remanence SIRM(T) or remanence imposed at  
45 different field strength in three perpendicular directions are also applied. These measurements  
46 provide unblocking temperature values ( $T_{ub}$ ) at which remanence carried by particular  
47 magnetic phase is completely lost.  $M(T)$  and  $k(T)$  curves are disturbed by alteration of  
48 magnetic phases during heating. Compared with  $M(T)$ ,  $k(T)$  curves are controlled not only by  
49 magnetic mineralogy but also by grain size distribution. SIRM(T) curves although affected by

50 grain size distribution, are not disturbed by mineralogical changes induced by heating.

51 Thermal alteration are detected during second heating.

52 Thermal transformations of magnetic minerals occurring during susceptibility measurements  
53 often differ significantly from transformations observed during remanence experiments or  
54  $M(T)$  measurements. The differences are demonstrated in Figs. 1 and 2 showing several  
55 examples of  $k(T)$  and  $SIRM(T)$  curves for rocks and soil. The thermal behaviour of  
56 susceptibility ( $k$ ) was determined with a KLY-3S kappabridge with a CS-2 furnace device  
57 made by the AGICO (Czech Republic). Heating was performed in air. A sample is heated up  
58 to the maximum temperature of 700 °C and subsequently cooled to room temperature.

59 Thermal demagnetization of saturation isothermal remanence (SIRM) was carried out with  
60 the use of a device made by the TUS, Poland. SIRM was imparted on a sample in the field of  
61 9 T high enough to saturate hard magnetic minerals such as hematite or goethite, and  
62 measured during heating up to 700 °C in a magnetic screen.

63 As it is seen in Figs. 1 and 2, during heating in  $SIRM(T)$  and  $k(T)$  experiments different  
64 magnetic minerals were created at the end due to specific oxidation – reduction conditions  
65 different in both experiments. During  $M(T)$  or  $SIRM(T)$  measurements oxidation conditions  
66 prevail whereas during  $k(T)$  experiment reduction takes place.

67 Although susceptibility changes during heating process did not often provide us with  $T_c$   
68 values of magnetic minerals present in a fresh sample, they can be used to better  
69 understanding of transformations of the iron oxides present in rocks and soils occurring in  
70 reduction conditions. Little attention have been paid to analyze susceptibility changes at high  
71 temperature in relation to transformation of magnetic minerals in rocks although Tanikawa et  
72 al. (2008) used thermomagnetic susceptibility analysis of core samples from the Chelungpu  
73 fault in Taiwan to explain high values of magnetic susceptibility of fault rocks.

Figs. 1, 2
---------------

74 In environmental magnetism, monitoring of thermal transformations during  $k(T)$   
75 measurements is used by several authors to describe processes occurring in soil during  
76 pedogenesis or anthropogenic activities ( fires, archeological objects, pollution). Pedogenesis  
77 involves a complex series of post-depositional processes related to environmental parameters  
78 such as temperature, rainfall, pH or microbial activity. There is still much to learn about the  
79 pedogenic processes and their sensitivity to various climatic factors. It is known that in soil  
80 pedogenesis leads to breakdown of iron-bearing silicates and clays to produce oxyhydroxides  
81 and ferrihydrite. Iron hydroxides transform to ferrimagnetic oxides such as magnetite or  
82 maghemite through dehydration process and then to hematite at higher temperature (Cornell  
83 and Schwertmann, 2003, Maher, 1998). Several authors (for example Hanesch and Petersen,  
84 1999, Dearing et al., 2001) proposed second mechanism of formation of magnetite from  
85 ferrihydrite with the help of iron-reducing bacteria. Magnetite is converted to maghemite  
86 through low-temperature oxidation. In nature according to Longworth et al.(1979) this  
87 mineral is neither magnetite nor maghemite, but solid solution between them, a cation-  
88 deficient magnetite. Özdemir and Banerjee (1982) studying Minnesota topsoil concluded that  
89 magnetite is the first strongly magnetic iron oxide produced in pedogenesis. Its concentration  
90 and small grain size of superparamagnetic range was responsible for susceptibility  
91 enhancement. Magnetite is slowly oxidized in ambient temperature to cation-deficient form  
92 and to maghemite at the end. Low-temperature oxidation of magnetite to maghemite is  
93 related to paleoclimate conditions and the degree of pedogenesis. Anthropogenic activity is  
94 usually connected with coarse- grained magnetite or hematite.

95 Temperature dependence of magnetic susceptibility has been widely used to determine  
96 mineralogy, grain size distribution and stoichiometry of magnetic assembly present in  
97 loess/paleosol sequence because it can help better understand pedogenic processes and link  
98 them to paleoclimate (Deng et al., 2001, Liu et al., 2004, 2005, 2007). Deng et al. (2001)

99 investigated magnetic mineralogical changes during thermal treatment of Holocene samples  
100 from the Chinese Loess Plateau. The results suggested the stronger pedogenesis caused the  
101 higher low-temperature oxidation, the higher content of maghemite, greater susceptibility  
102 decrease at 300–400 °C and weaker susceptibility peak at about 510°C. Lui et al. (2005)  
103 examined temperature dependence of susceptibility in argon of Chinese loess/paleosol and  
104 stated that the susceptibility loss during heating at temperature 300–400 °C is caused by the  
105 inversion of pedogenic fine-grained maghemite to hematite. They proposed that the  
106 susceptibility loss can be used as a new concentration index of pedogenic SP grains. They  
107 suggested that heating up to 700 °C in argon could be in some sense an analogue to the  
108 pedogenic processes. According to Liu et al.(2005) “ the effect of pedogenesis and thermal  
109 treatment on the bulk susceptibility seems to be equivalent...there exists a similarity in two  
110 aspects. First, the pedogenesis occurs in a reducing environment. Secondly, the pedogenesis  
111 produces a fine-grained assemblage (SP+SD)”. Maher et al. (2003a, 2003b) examined  
112 pedogenic susceptibility enhancement in soil of Russian steppe and in Chinese Loess Plateau  
113 in relation to rainfall. Banerjee (2006) outlined the problem of evaluation separately the role of  
114 abiotic and biotic reduction activity in formation of magnetic enhancement in soil. He  
115 believes that this enhancement may be a signature not only of paleorainfall but also of  
116 concentration of iron reducing bacteria species and their activity.

117 In the present paper we focus on the study of thermal transformations of iron oxides and  
118 oxyhydroxides in soil which take place during susceptibility measurements. Our interest in  
119 the problem arose from the central role they played in environmental magnetic and  
120 paleoclimatic study in deciphering of the environmental control on magnetic susceptibility  
121 enhancement in topsoil. In our earlier paper (Kopcewicz et al, 2006) we reported the results of  
122 Mössbauer spectroscopy used to identify iron oxides responsible for soil magnetism and for  
123 changes of the shape of magnetic susceptibility curves observed in the thermomagnetic

124 measurements. The first results justified the use of the laboratory heating process as a means  
125 to determine the thermal conversion of iron compounds in the different soil layers and  
126 eventually elucidate the problem of the influence of the organic matter on chemical processes  
127 which take place during heating.

128

## 129 EXPERIMENTS

130 The samples were taken from the Ukrainian chernozem soil profile from the Homutovsky  
131 Steppe reserve from the topsoil layer 0-10 cm of depth and from the loess layer 120–130 cm  
132 of depth. Table 1 shows chemical characteristics of the samples. They differ in humus content  
133 and progress of pedogenesis.

Table 1
---------

134 For identification of magnetic minerals the heating curves of saturation magnetization  $J_s(T)$   
135 and saturation remanence SIRM(T) were used. The saturation magnetization  $J_s(T)$  decay  
136 curves were measured with the means of a vibrating sample magnetometer in a field of a  
137 strength of 0.45 T from 20 °C to 700 °C in paleomagnetic laboratory of the Institute of  
138 Physics of the Earth in Moscow. For the topsoil sample the saturation remanence decay curve  
139 SIRM(T) during heating showed a phase with  $T_{ub} \sim 630$  °C which we interpret as maghemite  
140 (Fig. 2). The  $J_s(T)$  curve reveals mineral of  $T_c$  below 700 °C and weak increase at  
141 temperature of about 500 °C indicates formation of small amount of new magnetite. The  $T_c$   
142 and  $T_{ub}$  were determined from heating curve by the two- tangent method proposed by  
143 Grommé et. al. (1969). Magnetic measurements were completed by Mössbauer analysis  
144 which shows the presence of maghemite, hematite and goethite. For the loess sample,  $T_{ub}$  and  
145  $T_c$  are about 690 °C. Mössbauer analysis shows hematite associated with some amount of  
146 maghemite and goethite (Kopcewicz et al., 2005).

147 In the case of our samples the heating curves of  $k(T)$  demonstrate several mineral  
148 transformations (Fig.2). The most common explanation of these curves is as follows: the first



149 small increase of susceptibility at about 220 °C (for the topsoil sample) and 300 °C (for the  
150 loess sample) represents dehydration of goethite to hematite. The drop of  $k$  between 220 °C  
151 and 400 °C or 300 °C and 450 °C, for the topsoil and the loess respectively, is due to  
152 transformation of maghemite to hematite. Formation of new magnetite starts from 400 - 450  
153 °C. The Curie temperature determined from heating curve is about 590 °C by the two- tangent  
154 method proposed by Grommé et. al. (1969) or 570 °C according to the method proposed by  
155 Petrovsky and Kapička (2006). Both pointed to magnetite as the main magnetic mineral. The  
156 increase of room susceptibility after heating up to 700 °C is 2.6 times for the topsoil and 20  
157 times for the loess. It should be noted that in the loess, only small part of magnetite was  
158 created below 600 °C. Formation of magnetite occurred predominately above 600 °C. For the  
159 topsoil thermally induced mineral changes make impossible determination of the Curie  
160 temperature of original minerals. Even for the loess when the changes of  $k$  seems moderate up  
161 to 600 °C, the Curie temperature determined from heating curve do not represent the original  
162 magnetic mineral but is disturbed by newly formed magnetite.

163 To document the sequence of magnetic mineral transformations during the heating process  
164 the set of experiments was performed. The scheme of experiments is illustrated in Fig.3. The  
165 sample of soil was divided into 5 specimens. Each specimen was heated in KLY-3 device up  
166 to different increasing temperature: 250 °C, 400 °C, 500 °C, 600 °C and 700 °C. After  
167 heating, low temperature experiments, SIRM(T) curves, hysteresis loops and Mössbauer  
168 analysis were performed for each specimen.

Fig. 3

169 The susceptibility behaviour during heating was shown in Fig. 4. For the topsoil sample  
170 small alteration occurs after heating up to 250 °C. Dramatic transformation starts at 500 °C,  
171 with maximum at 600 °C. For the loess, alteration starts at 400 °C, susceptibility increases  
172 slowly with temperature and shows enormous increase after heating up to 700 °C.

Fig. 4

173 To quantify the degree of irreversibility of thermomagnetic curves, we used the alteration  
 174 factor  $A(40)$  introduced by Hrouda (2003) to characterize the irreversible changes of  $k$ . The  
 175  $A(40)$  index was defined by Hrouda (2003) as follows:  $A(40) = 100(k_{Tc,40} - k_{Th,40})/k_{Th,40}$ ,  
 176 where  $k_{Tc,40}$  and  $k_{Th,40}$  are values of total susceptibility at 40 °C during cooling and heating,  
 177 respectively. The  $A(40)$  index described above is shown in Fig.5a. As grain size influence  
 178 magnetic susceptibility, especially in the range of fine grains, the amount of newly generated  
 179 strong magnetic phases is better represented by ferrimagnetic contribution to  $M_s$  (Fig.5b)  
 180 calculated from hysteresis loop. The both parameters follow similar courses but the increase  
 181 of ferrimagnetic content is not so dramatic as in the case of susceptibility. This situation can  
 182 be explained by creation of SP grains at high temperature which influences strongly magnetic  
 183 susceptibility.

Fig. 5

184 SIRM(T) curves of heated specimens (Fig.6) show that significant amount of magnetite was  
 185 created after heating up to 500 °C in the topsoil samples and after heating up to 700 °C in the  
 186 loess samples. The “drops” at about 200 °C on SIRM(T) curves obtained for samples  
 187 previously after heated up to 500°C in  $k(T)$  experiment are related to structural features rather  
 188 than to magnetic phases. They are not seen on  $k(T)$  curves and because of that can be interpreted  
 189 as unblocking of unstable remanence carried by fine grains of size just above SD/SP  
 190 boundary.

Fig. 6

191 Low-temperature dependence of susceptibility was measured by means of a KLY-3S  
 192 Kappabridge with a CSL cryostat device made by the AGICO (Czech Republic) during  
 193 warming samples from the liquid nitrogen temperature (LNT = -196° C) up to room  
 194 temperature. Susceptibility varies with temperature in complicated manner depending on  
 195 magnetic mineralogy and also on grain size. Low-temperature experiments provide  
 196 information about the presence of magnetite and hematite if the Verwey or Morin transitions  
 197 are observed. The shape of low-temperature curves can provide information about the

Fig. 7

198 contribution of paramagnetic or superparamagnetic grains to the bulk susceptibility  
199 (Thompson and Oldfield, 1986; Eyre and Shaw, 1994). Fig. 7 shows low-temperature curves  
200 for the topsoil and the loess samples heated previously up to temperatures: 250 °C, 400 °C,  
201 600 °C and 700 °C. For the topsoil, first changes were observed for the sample heated up to  
202 400 °C when Verwey transition was marked and the shape of curve becomes SD like. For  
203 sample heated up to 600 °C and to higher temperatures the curves look like SP behaviour and  
204 they differ from that for unheated soil only by presence of magnetite marked by the Verwey  
205 transition and higher value of susceptibility. For the loess, first changes were observed after  
206 heating to 600 °C when the concave shape of curve becomes almost linear. For the sample  
207 heated up to 700 °C, increase of susceptibility and the lack of Verwey transition is an  
208 evidence of the presence of SP grains. This observation agrees with our interpretation of  
209 variations of the A(40) index and ferromagnetic contribution to  $M_s$ .

210 Hysteresis parameters were measured by means of Micro-Mag, AGM device produced by  
211 Princeton Measurements Corp. USA with maximum field of 1.4T (Table 2). For the topsoil  
212 sample, heating caused increase of  $M_s$ ,  $M_r$ ,  $H_c$  and  $H_{cr}$  starting from temperature of 400 °C  
213 with the maximum increase after heating up to 600 °C. For the loess sample,  $M_s$  and  $M_r$  begin  
214 to increase after heating up to 500 °C with the biggest increase after heating up to 700 °C.  $H_c$   
215 and  $H_{cr}$  decreased. In general, after the heating process, hysteresis parameters, ratios  $M_r/M_s$   
216 and  $H_{cr}/H_c$  (Table 2) indicate greater contribution of fine grains in heated samples than in  
217 fresh material (Day et al., 1977). The contribution of soft and hard material in the topsoil and  
218 the loess during heating is demonstrated by the ratio of hysteresis parameters of the topsoil to  
219 the respective parameters of the loess (Table 2). In fresh material, the contribution of soft and  
220 strong minerals is greater in the topsoil than in the loess whereas at the end of the heating  
221 process the loess sample contains more such minerals.

Table 2

Fig. 8, 9

222 To change the conditions of experiment we applied different mode of heating. The sample of  
223 topsoil and the sample of loess were heated in so-called “multi-heating cycles” up to  
224 increasing temperatures; 250, 400, 500, 600 and 700 °C in Czech KLY -3S device. The  
225 sample was heated up to 250 °C and cooled to room temperature, then heated again to 400 °C  
226 and cooled again to room temperature. The heating was repeated up to 700 °C. Changes of  
227 susceptibility during succeeding heatings were shown in Fig. 8. When compared with the  
228 results of previous experiments one can see that in the case of the topsoil the changes are of  
229 similar character only on a smaller scale (Fig. 5b). The loess sample also exhibits similar  
230 changes of  $k$  until heating up to 400 °C (Fig.8). During heating to higher temperature  $k(T)$   
231 curves become almost reversible (Figs. 9 and 5b) with the Curie temperature above 600 °C.  
232 SIRM(T) curve of heated topsoil sample shows “decline” at temperature below 200 °C not  
233 observed on SIRM(T) curve for fresh sample. For the loess, SIRM(T) curves are practically  
234 similar for fresh and heated samples.

235

## 236 MÖSSBAUER MEASUREMENTS

237 To verify the results obtained during magnetic measurements the Mössbauer spectroscopy  
238 was used. Mössbauer measurements were performed for the fresh topsoil and loess samples,  
239 for samples heated up to  $T = 250, 400, 500, 600$  and  $700$  °C (each time starting from room  
240 temperature) and for samples heated up to  $700$  °C in multi-heating process.

241 First results of the Mössbauer analyses of soil samples heated during measurements of the  
242 magnetic susceptibility were reported by Kopcewicz et al.(2006).

243 The Mössbauer parameters obtained for fresh samples revealed the presence of  $Fe^{3+}$  ions in  
244 paramagnetic minerals represented by two paramagnetic doublets. One doublet with isomer  
245 shift  $\delta = 0.36$  mm/s and quadrupole splitting  $\Delta = 0.43$  mm/s represented group of minerals  
246 named A, and the doublet with  $\delta = 0.37$  mm/s and  $\Delta = 0.93$  mm/s represented group of

Table 3

247 minerals called B. The  $\text{Fe}^{2+}$ -bearing silicate minerals were represented by paramagnetic  
248 doublet with  $\delta = 1.08$  mm/s and  $\Delta = 2.74$  mm/s. Taking into account the value of hyperfine  
249 parameters, the paramagnetic doublets (A and B) may originate from  $\text{Fe}^{3+}$  cations in the  
250 oxyhydroxides (ferrihydrite,  $\beta$ -FeOOH and  $\gamma$ -FeOOH), from silicates and/or from iron-  
251 containing antiferromagnetic and ferrimagnetic iron oxides in the form of ultra fine particles  
252 in superparamagnetic state. Kopcewicz et al. (2005) verified the origin of the quadrupole  
253 doublets by performing the Mössbauer measurements at 80 K (LNT) and the results suggested  
254 that some part of iron oxides may appeared in the form of ultra fine particles in the  
255 superparamagnetic state. Part of  $\text{Fe}^{3+}$  cations (B) together with  $\text{Fe}^{2+}$  cations comes most  
256 probably from clay minerals. Also magnetically ordered iron oxides ( $\alpha$ - $\text{Fe}_2\text{O}_3$ ,  $\alpha$ -FeOOH,  $\gamma$ -  
257  $\text{Fe}_2\text{O}_3$ ) were identified in the samples. The approximate mineralogical content was determined  
258 by relative area (RA) of the Mössbauer spectral components corresponding to each  
259 compound (Table 3).

260 Values of isomer shift and quadrupole splitting, for both minerals A and B, remain relatively  
261 similar for samples heated up to 250 °C. After heating up to temperatures higher than 250 °C  
262 we observed more pronounced increase in quadrupole splitting values characteristic of  
263 distorted crystalline coordination which suggests the beginning of dehydration process (loss  
264 of hydroxyl).

265 The  $\text{Fe}^{3+}$  cations in minerals described as A which contained OH and/or structural water were  
266 significantly affected by the heating. Their content significantly decreases. Ferric and ferrous  
267 iron present as structural iron in silicates (minerals B) was more stable. Simultaneously, a  
268 steady increase of  $\text{Fe}^{2+}$  cations content in the paramagnetic components was observed which  
269 indicates that transformation process occurred under reduction conditions.

270 The changes of relative iron content in paramagnetics and relative content of magnetic  
271 minerals for the heated topsoil and loess samples identified in the Mössbauer experiment are

272 shown in Table 3 and Fig. 10. Mössbauer analysis shows that goethite was broken up after  
273 heating up to 250°C. Maghemite in soil is extremely stable and transforms to hematite after  
274 heating up to 700 °C. In the topsoil sample, content of magnetite increases in the whole  
275 heating range. In the loess, magnetite was created by heating up to 400 °C and to 700 °C.  
276 However, the Mössbauer analysis made for the topsoil and loess samples heated up to 700 °C  
277 in multi-heating process give different picture of chemical changes. Fig. 11 and Tables 4 and  
278 5 show the differences in content of iron compounds depending on the way of heating  
279 process. For topsoil sample, in the case of multi-heating process chemical changes had the  
280 same character as in the case of single heating up to 700 °C. It was process of reduction and  
281 only amount of Fe<sup>2+</sup> cations (RA) both, in paramagnetic and magnetic compounds, increased.  
282 For loess sample, the chemical changes had completely different character during multi-  
283 heating process. The Mössbauer spectrum in Fig. 11c (right) consists of two paramagnetic  
284 doublets (Fe<sup>3+</sup> in minerals A and B), a six line spectrum with the Mössbauer parameters  
285 (Table 5) which corresponds to hematite and a weak sextet which likely corresponds to Fe<sup>3+</sup>  
286 cations in maghemite. The Fe<sup>2+</sup> cations disappeared completely. It suggests oxidation  
287 character of the chemical changes in the loess sample during multi-heating process.

288

## 289 DISCUSSION

290 The susceptibility enhancement in the topsoil is due to formation of strong ferrimagnetic  
291 oxides magnetite/maghemite as an effect of pedogenesis.  
292 Pedogenesis starts from weathering of paramagnetic mother clay minerals, amphibolites etc.  
293 to form ferrihydrite, and amorphous oxyhydroxide containing Fe<sup>3+</sup> iron. This iron is reduced  
294 to Fe<sup>2+</sup> by “fermentation” process according to LeBorgne (1960) or due to iron-reducing  
295 bacteria (Banerjee, 2006) and combined with the remaining Fe<sup>3+</sup> ions to form fine-grained  
296 magnetite. Finally, magnetite is oxidized to maghemite. Barron and Torrent, (2002) proposed

297 another mechanism for maghemite creation— slow transformation of ferrihydrite to maghemite  
298 at near ambient temperature. Another possibility is dehydroxylation of lepidocrocite which  
299 can also lead to maghemite formation. During pedogenesis goethite and hematite are also  
300 produced. As a result, topsoil contains goethite and hematite, both pedogenic and lithogenic,  
301 fine-grained magnetite and/or maghemite. In well developed soil, for example in the Chinese  
302 Loess Plateau, strong ferrimagnetic mineral is neither pure magnetite nor pure maghemite but  
303 partly oxidized magnetite.

304 The results of our experiments show that in our samples the starting minerals which can play  
305 role in magnetic transformations are iron oxides - maghemite and hematite determined from  
306 SIRM(T) curves and from the Mössbauer spectrum. Additionally, hydroxides such as  
307 goethite, lepidocrocite (?) and ferrihydrite and amorphous structurally iron- bearing  
308 oxyhydroxide were found from the Mössbauer analysis. Although the set of magnetic  
309 minerals is the same for both samples, and the content of hematite is similar, the topsoil  
310 contains more maghemite and goethite than the loess. SIRM(T) curves and the Mössbauer  
311 analysis revealed that the fresh material of both samples did not contain magnetite.

312 According to Liu et al.(2005), the absence of magnetite is a demonstration of the maturity of  
313 our soil.

314 The Mössbauer analysis showed that during thermal experiment (Fig. 10), goethite was  
315 dehydrated after heating up to 250 °C, and should transform to maghemite and/or hematite.  
316 However, we did not observe increase of these minerals content. For the topsoil, at that  
317 temperature small amount of magnetite was created. Özdemir and Dunlop (2000) found that  
318 during dehydration of goethite intermediate spinel phase - magnetite was formed. This  
319 process can be responsible for magnetite appearance in the topsoil sample. In the loess,  
320 thermal transformation of goethite can occur in a different way. Przepiera and Przepiera  
321 (2003) have proved that dehydroxylation of precipitated goethite begins at temperature of 200

322 °C by conversion into amorphous form of hematite (protohematite). As reducing conditions  
323 prevail during experiment, after heating up to 400 °C magnetite is created. We observed  
324 decrease of susceptibility between 300 – 400 °C. Usually this decrease is explained by  
325 conversion of pedogenic maghemite to hematite ( Liu et al. 2005). However, the SIRM(T)  
326 curves and the Mössbauer analysis did not confirm conversion of maghemite to hematite at  
327 temperature range of 300 – 400 °C. Complete conversion of maghemite is observed for both  
328 samples at much higher temperature after heating up to 700 °C. We explained the loss of k  
329 between 300 and 400 °C as a result of increase of grain size from SP to SD on the basis of  
330 low – temperature experiments. In the topsoil, production of magnetite was continued during  
331 subsequent heatings. For the loess, magnetite was created at 400 °C and then at 600 °C and  
332 higher. According to Cornell and Schwertmann (2003) magnetite can be generated through  
333 reduction from lepidocrocite, ferrihydrite and hematite. Barron et al. (2003) proposed that in  
334 soil after heating up to 400° C ferrihydrite converts to magnetite and maghemite. Such  
335 processes, besides transformation of goethite, can be responsible for production of magnetite  
336 at the whole range of temperature in the topsoil and at 400 °C in the loess. Hanesch et al.  
337 (2006) studying thermal transformations of goethite, lepidocrocite and ferrihydrite found that  
338 the transformations start between 200 and 350 °C for ferrihydrite and lepidocrocite and  
339 around 450 °C for goethite. They observed that the presence of organic carbon leads to  
340 formation of maghemite or magnetite instead of hematite which is created without organic  
341 carbon. In the case of lepidocrocite, organic carbon decreases the transformation temperature  
342 and intensifies the effect. The presence of organic carbon intensifies conversion of hematite to  
343 magnetite. We observed that in the topsoil the presence of humus lowers temperature at which  
344 the increase of Fe<sup>2+</sup> content and formation of magnetite starts. The temperatures of  
345 transformation found by Hanesch et al. (2006) are a little higher than in our experiment. In the  
346 loess, organic matter is almost absent. However, the reducing conditions prevail also in the



347 loess (Table 1). At 700 °C reduction of hematite leads to production of magnetite. In spite of  
348 lack of humus, the increase of susceptibility at the end of the heating process is much higher  
349 in the loess than in the topsoil (Fig. 5).

350 When we have compared  $M_r$  and  $M_s$  intensities for the both samples (Table 2) at the end of  
351 experiment, the absolute values turned out to be almost equal. The increase of  $M_r$  and  $M_s$   
352 caused by the heating process was expressed by the values of remanent and saturation  
353 magnetizations ratios measured at room temperature ( $M_r(RT)$ ,  $M_s(RT)$ ), and after heating up  
354 to 700 °C ( $M_r(700)$  and  $M_s(700)$ ). The enhancement (Table 2) is much higher for the loess (33  
355 and 29.5, respectively) than for the topsoil (12.8 and 8.5, respectively) and higher for  $M_s$  than  
356 for  $M_r$ . The difference between the enhancement in the loess and in the topsoil can be related  
357 to the degree of pedogenesis. The difference between the enhancement of  $M_r$  and  $M_s$  can be  
358 related to the important contribution of SP grains in loess heated previously to 700 °C. It is  
359 confirmed by the shape of  $k(T)$  curve obtained in low-temperature experiment.

360 The high stability of maghemite which converts to hematite at the very high temperature of  
361 700 °C in the both samples – topsoil and loess - is rather unusual for this mineral. Although  
362 such high temperature of inversion was reported for loess (Liu et al. 2003) or synthetic  
363 samples (Özdemir and Banerjee, 1984), de Boer and Dekkers (1996) found that the coarser  
364 grains, the higher inversion temperature appears. Liu et al. (2005, 2007, Deng et al., 2001)  
365 reported inversion temperature of maghemite about 300–400 °C. They correlated the  
366 decrease of susceptibility caused by this process with the degree of pedogenesis. Hanesch et  
367 al. (2006) stated that maghemite obtained from goethite in the presence of organic carbon  
368 does not transform to hematite when heated up to 800 °C. Also Liu et al. (2004) found in  
369 Chinese loess/paleosol maghemite which was stable till 700 °C. They stressed that partly  
370 oxidized magnetite often occurring in loess/paleosol have different magnetic properties than  
371 its fully oxidized form – maghemite.

372 The topsoil and loess in our study do not differ significantly in such pedogenic parameters as  
373 pH, total iron content  $Fe_t$  or free iron  $Fe_d$ . The main differences are in humus and amorphous  
374 iron content  $Fe_o$  (Table 1). Smaller content of  $Fe_o$  indicates less amount of ferrihydrite in the  
375 loess than in the topsoil. Almost equal values of  $M_r$  and  $M_s$  for the both samples at the end of  
376 the heating process suggest that pedogenic formation of strong ferrimagnetic minerals  
377 observed in the topsoil is limited by the amount of iron in a parent material.

Fig. 11

378 The multi-heating experiment indicated that humus play important role in keeping reduction  
379 conditions during succeeding heatings. For the loess, reduction conditions were held only at  
380 the beginning of experiments during two first heating runs. We suggest that reduction  
381 conditions were held due to evaporation of water present in a sample. The oxygen access was  
382 hindered by the vapor formed during heating. The observed differences between behaviour of  
383 the topsoil and the loess samples during multi-heating process can be explain by different  
384 content of organic matter in the samples. In the case of the topsoil humus keeps sufficient  
385 amount of water whereas in the loess water is barely enough for two first heating runs. In the  
386 case of topsoil the reduction atmosphere is more stable and lasts longer than in the case of the  
387 loess layer where the content of organic matter is limited. In the loess sample the multi-  
388 heating process changes the atmosphere from reduction to oxidation which has the essential  
389 influence on final results of the chemical processes.

390 Summarizing, as the topsoil and loess contain similar amount of hematite we suggest  
391 predominantly lithogenic origin of this mineral. The enhanced amount of goethite in the  
392 topsoil indicates that the great part of goethite has pedogenic origin probably in association  
393 with ferrihydrite in moderate and wet climate. Among the pathway of maghemite formation,  
394 oxidation of magnetite is the less probable as no magnetite was revealed in fresh samples.  
395 High thermal stability of maghemite points to poor crystallized, transitional form originated

396 from goethite or ferrihydrite. The role of magnetotactic or iron-reducing bacteria seems  
397 rather marginal.

398

#### 399 CONCLUSIONS

400 The experiment can help to trace the alterations of magnetic oxides and hydroxides occurring  
401 during the heating process and to determine temperatures at which different transformations  
402 take place. The Mössbauer analysis proved that reduction conditions are held during k(T)  
403 measurements performed in the Czech KLY –3S device. In single heating process at low  
404 temperature of 200 – 450°C, the prevailing transformations are thermal dehydration/  
405 dehydroxylation of hydroxides such as goethite, lepidocrocite and ferrihydrite to  
406 magnetite/maghemite, whereas at temperature above 600°C reduction of hematite is the main  
407 source of new magnetite. In the topsoil the first process is more important whereas in the  
408 loess reduction of hematite to magnetite prevails. The difference in the enhancement of  
409 magnetization in the loess and the topsoil can be related to the degree of pedogenesis. The  
410 unusual stability of maghemite can be ascribed to specific climate conditions but this  
411 suggestion needs confirmation by further study of soil from different climatic zones. The  
412 multi-heating process in loess sample change the reduction atmosphere to oxidation one and  
413 at the end of thermal transformation only Fe<sup>3+</sup> bearing compounds were observed. The humus  
414 plays important role in keeping reduction atmosphere during the heating process due to  
415 enough amount of bounded water.

416

#### 417 ACKNOWLEDGEMENTS.

418 The study was performed in the Institute of Geophysics of Polish Academy of Sciences,  
419 Poland in the frame of the program 7/2006 of the Institute of Geophysics, PAS. We are

420 grateful to prof. M. Kopcewicz ( Institute of Electronic Materials Technology, Warsaw,  
421 Poland) for his help in measurement of the Mössbauer spectra.

422

#### 423 REFERENCES

424 Banerjee, S.K., 2006. Environmental magnetism of nanophase iron minerals: testing the  
425 biomineralization pathway. *Phys. Earth. Planet. Int.* 154, 210-221.

426 Barrón, V., Torrent, J., 2002. Evidence for a simple pathway to maghemite in Earth and Mars  
427 soils. *Gochim. Cosmochim. Acta.* 66, 2801-2806.

428 Barrón, V., Torrent, J., de Grave, E., 2003. Hydromaghemite, an intermediate in the  
429 hydrothermal transformation of 2-line ferrihydrite into hematite. *American  
430 Mineralogist.* 88, 1679-1688.

431 Cornell, R.M., Schwertmann, U., 2003. *The iron oxides.*, Wiley-VCH Gmbh&Co. KgaA,  
432 Weinheim

433 Day, R., Fuller M., Schmidt .A, 1977. Hysteresis properties of titanomagnetite: Grain size  
434 and composition dependence. *Phys. Earth. Planet. Int.* 13, 260-267.

435 Dearing, H.A., Hannam, J.A., Anderson, A.S., Wellington, E.M.H., 2001. *Geophys. J.*  
436 *Int.*144, 183-196.

437 De Boer, C.B., Dekkers, M.J., 1996. Grain size dependence of the rock magnetic properties  
438 for a natural maghemite. *Geophys. Res. Lett.* 23, 2815-2818.

439 Deng, C., Jackson, M.J., Verosub, K.L., Singer, M.J., 2001. Variability of the Temperature-  
440 Dependent susceptibility of the Holocene Eolian Deposits in the Chinese Loess  
441 Plateau: A Pedogenesis indicator. *Phys. Chem. Earth (A).* 26, No. 11-12, 873-878.

442 Eyre, J.K., Shaw, J., 1994. Magnetic enhancement of Chinese loess – the role of  $\gamma\text{Fe}_2\text{O}_3$ .  
443 *Geophys. J. Int.* 117, 265-271.

- 444 Grommé, C.S., Wright, T.L., Peck, D.L., 1969. Magnetic properties and oxidation of iron-  
445 titanium oxide minerals in Alae and Makaopuhi lave lakes, Hawaii. *J. Geophys. Res.*  
446 74, 527-5293.
- 447 Hanesch, M., Petersen, N., 1999. Magnetic properties of recent parabrown-earth from  
448 Southern Germany. *Earth Planet. Sci. Lett.* 169, 85-97.
- 449 Hanesch, M., Stanjek, H., Petersen, N., 2006. Thermomagnetic measurements of soil iron  
450 minerals: the role of organic carbon. *Geophys. J. Int.* 165, 53-61.
- 451 Hrouda, F., 2003. Indices for numerical characterization of the alteration processes of  
452 magnetic minerals taking place during investigation of temperature variation of  
453 magnetic susceptibility. *Stud. Geophys. Geod.* 47, 847-861.
- 454 Kopcewicz, B., Kopcewicz, M., Jeleńska, M., Hasso-Agopsowicz, A., 2005. Mössbauer  
455 Study of Soil Profiles in industrial region of Ukraine. In: *Industrial Applications of*  
456 *the Mössbauer Effect*. eds: M. Garcia, J. F. Marco, and F. Plazaola, American  
457 Institute of Physics, Melville, New York, 378-383.
- 458 Kopcewicz, B., Kopcewicz, M., Jeleńska, M., Hasso-Agopsowicz, A., 2006. Mössbauer  
459 study of chemical transformations in soil samples during thermomagnetic  
460 measurements. *Hyperfine Interact.* DOI 10.1007/s10751-006-9332-3.
- 461 LeBorgne, E., 1960. Influence du feu sur les propriétés magnétiques du sol et sur celles du  
462 schiste et du granite. *Annales de Géophysique.* 16, 159-195.
- 463 Longworth, G., Becker, L.W., Thompson, R., Oldfield, F., Dearing, J.A., Rummery, T.A.,  
464 1979. Mössbauer effect and magnetic studies of secondary iron oxides in soils. *J. Soil*  
465 *Sci.* 30, 93-110.
- 466 Liu, Q.S., Banerjee, S.K., Jackson, M.J., Chen, F.H., Pan, Y.X., Zhu, , R.X., 2003. An  
467 integrated study of the grain-size dependent magnetic mineralogy of the Chinese

- 468 loess/paleosol and its environmental significance. *J Geophys. Res.* 108, 2437, doi:  
469 10.1029/2002JB002264.
- 470 Liu, Q.S., Banerjee, S.K., Jackson, M.J., Deng, Ch., Pan, Y.X., Zhu, , R.X., 2004. New  
471 insights into partial oxidation model of magnetites and thermal alteration of magnetic  
472 mineralogy of the Chinese loess in air. *Geophys. J. Int.* 158, 506-514.
- 473 Liu, Q.S., Deng, Ch., Yu, Y., Torrent, J., Jackson, M.J., Banerjee, S.K., Zhu, , R.X., 2005.  
474 Temperature dependence of magnetic susceptibility in an argon environment:  
475 implications for pedogenesis of Chinese loess/palaeosol. *Geophys. J. Int.* 161, 102-  
476 112.
- 477 Liu, Q.S., Deng, Ch., Torrent, J., Zhu, , R.X., 2007. Review of recent developments in  
478 mineral magnetism of the Chinese loess. *Quat. Sci. Rev.* 27, 368-385.
- 479 Maher, B.A., 1998. Magnetic properties of modern soils and Quaternary loessic/paleosol:  
480 paleoclimatic implications. *Palaeogeogr. Palaeoclimatol. Palaeoecol.* 37, 25-54.
- 481 Maher, B.A., Alekseev, A., Alekseeva, T., 203a. Magnetic mineralogy of soil across the  
482 Russian Steppe: climatic dependence of pedogenic magnetic formation. *Palaeogeogr.*  
483 *Palaeoclimatol. Palaeoecol.* 201, 321-341.
- 484 Maher, B.A., Hu, M.Y., Roberts, H.M., Wintle, A.G., 2003b. Holocene loess accumulation  
485 and soil development at the western edge of the Chinese Loess Plateau: implications  
486 for magnetic proxies of paleorain-fall. *Quat. Sci. Rev.* 22, 445-451.
- 487 Özdemir, Ö., Banerjee, S.K., 1982. A preliminary magnetic study of soil samples from west-  
488 central Minnesota. *Earth Planet. Sci. Lett.* 59, 393-403.
- 489 Özdemir, Ö., Banerjee, S.K., 1984. High temperature stability of maghemite. *Geophys. Res.*  
490 *Lett.* 11, 161-164.
- 491 Özdemir, Ö., Dunlop, D.J., 2000. Intermediate magnetite formation during dehydration of  
492 goethite. *Earth Planet. Sci. Lett.* 177, 59-67.

- 493 Petrovsky, E., Kapička, A., 2006. On determination of the Curie point from thermomagnetic  
494 curves. *J. Geophys. Res.* 111, B12S27, doi: 10.1029/2006JB004507.
- 495 Przepiera, K., Przepiera, A., 2003. Thermal transformations of selected transition metals  
496 oxyhydroxides. *J. Therm. Anal. Ca.* 74, 659-666.
- 497 Tanikawa, W., Mishima, T., Hirono, T., Soh, W., Song S., 2008. High magnetic susceptibility  
498 produced by thermal decomposition of core samples from the Chelungpu fault in  
499 Taiwan. *Earth Planet. Sci. Lett.* 272, 372-381.
- 500 Thompson, R., Oldfield, F., 1986. *Environmental magnetism*. Allen & Unwin, London.

501

## 502 FIGURES CAPTION

503 Fig. 1. Examples of changes of susceptibility (left curves) and saturation remanence (right  
504 curves) during heating for rocks.  $k_1$  – room-temperature susceptibility for fresh sample;  $k_2$ –  
505 room-temperature susceptibility for heated sample. SIRM(1) - room-temperature saturation  
506 remanence for fresh sample; SIRM(2) - - room-temperature saturation remanence for heated  
507 sample.

508 Fig.2. Changes of susceptibility (a, b); decay curves of saturation remanence (c, d) and  
509 saturation magnetization (e, f) during heating for topsoil and loess samples, respectively.

510 Insets in left corner of a) and b) curves show full heating – cooling cycle of susceptibility  
511 variation. Legend as in Fig. 1.

512 Fig. 3. Scheme of experiments.

513 Fig. 4. Changes of susceptibility during heating of one specimen once to particular  
514 temperature ( 250°C, 400°C, 500°C, 600°C, 700 °C), for topsoil (left curves) and loess (right  
515 curves) samples.

516 Fig. 5. a) Parameter A(40) for samples of topsoil and loess heated in two modes. Full symbols  
517 – specimens heated once to particular temperature; open symbols – one specimen heated to  
518 increasing temperatures. Circles – topsoil; triangles – loess. b) Content of ferrimagnetic  
519 minerals calculated from hysteresis loop.

520 Fig. 6. Decay curves of SIRM(T) for samples of topsoil and loess heated once to particular  
521 temperature.

522 Fig. 7. Changes of susceptibility during warming from liquid nitrogen to room temperature  
523 for samples of topsoil and loess heated once to particular temperature.

524 Fig. 8. Changes of susceptibility during multi-heating of specimen to increasing temperatures:  
525 250°C, 400°C, 500°C, 600°C, 700 °C, for topsoil (left curves) and loess samples (right  
526 curves).

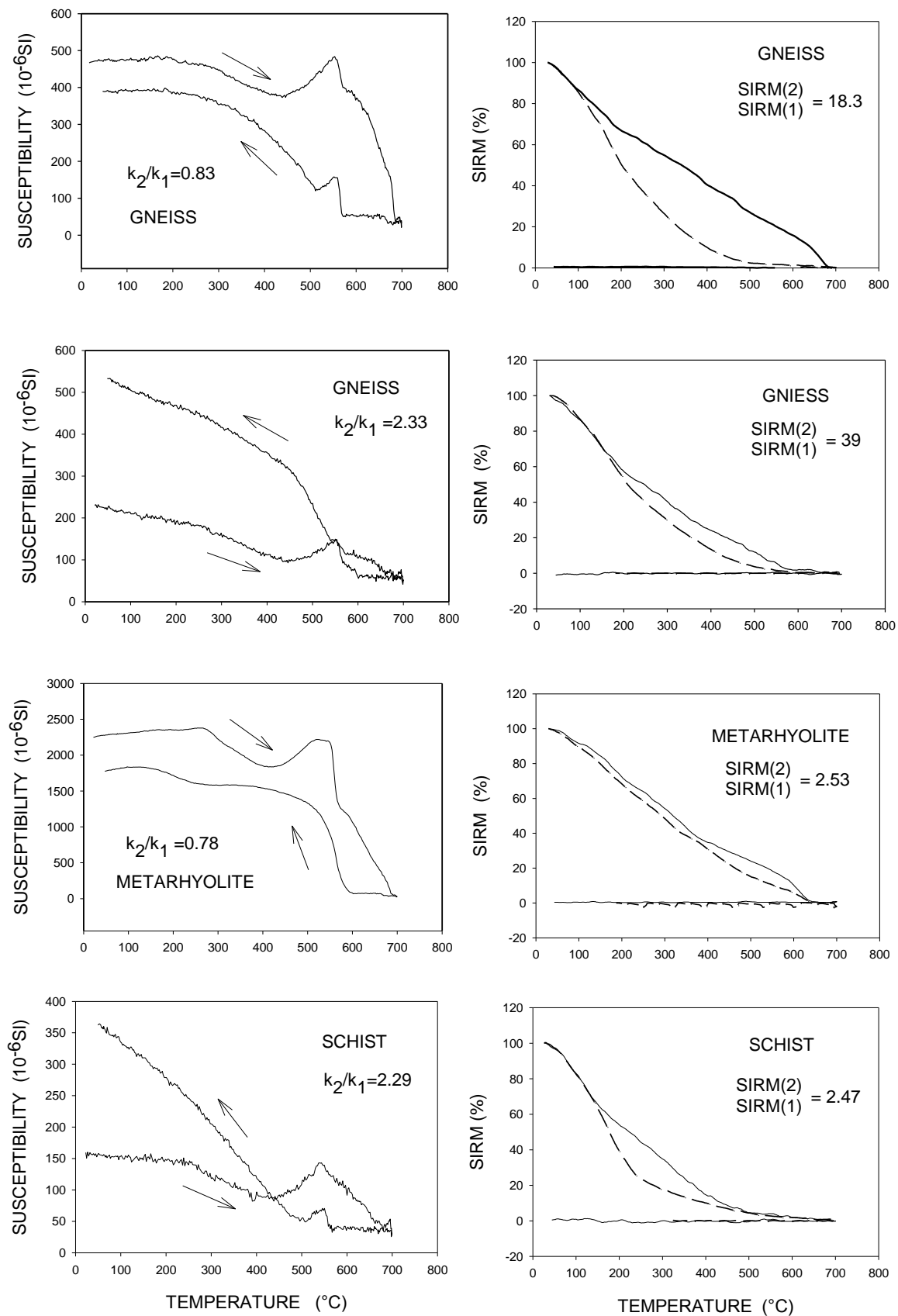
527 Fig. 9. Decay curves of SIRM(T) for: a) topsoil and b) loess samples heated previously  
528 several times to increasing temperatures (multi-heating process).

529 Fig. 10. Changes of iron content in paramagnetics (a, b) and in magnetic minerals (c, d) for  
530 samples of topsoil and loess heated to particular temperature from room temperature.

531 Fig. 11. Mössbauer spectra for the topsoil (left diagram) and loess (right diagram) samples  
532 measured at room temperature: a – for fresh sample; b – for sample heated from room  
533 temperature to 700 °C; c – for sample heated by multi-heating process to maximum  
534 temperature 700 °C.



Fig.1



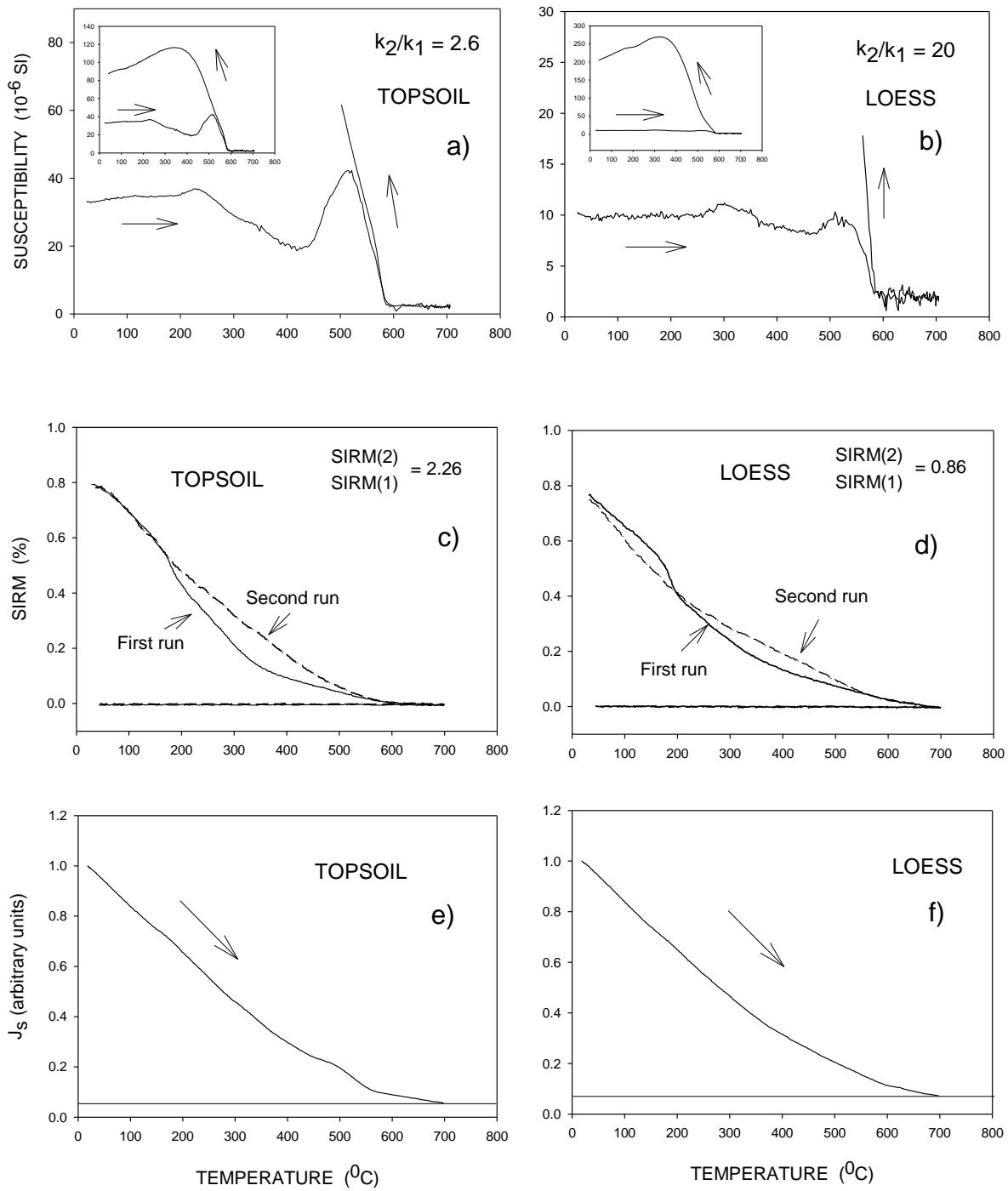


Fig. 2

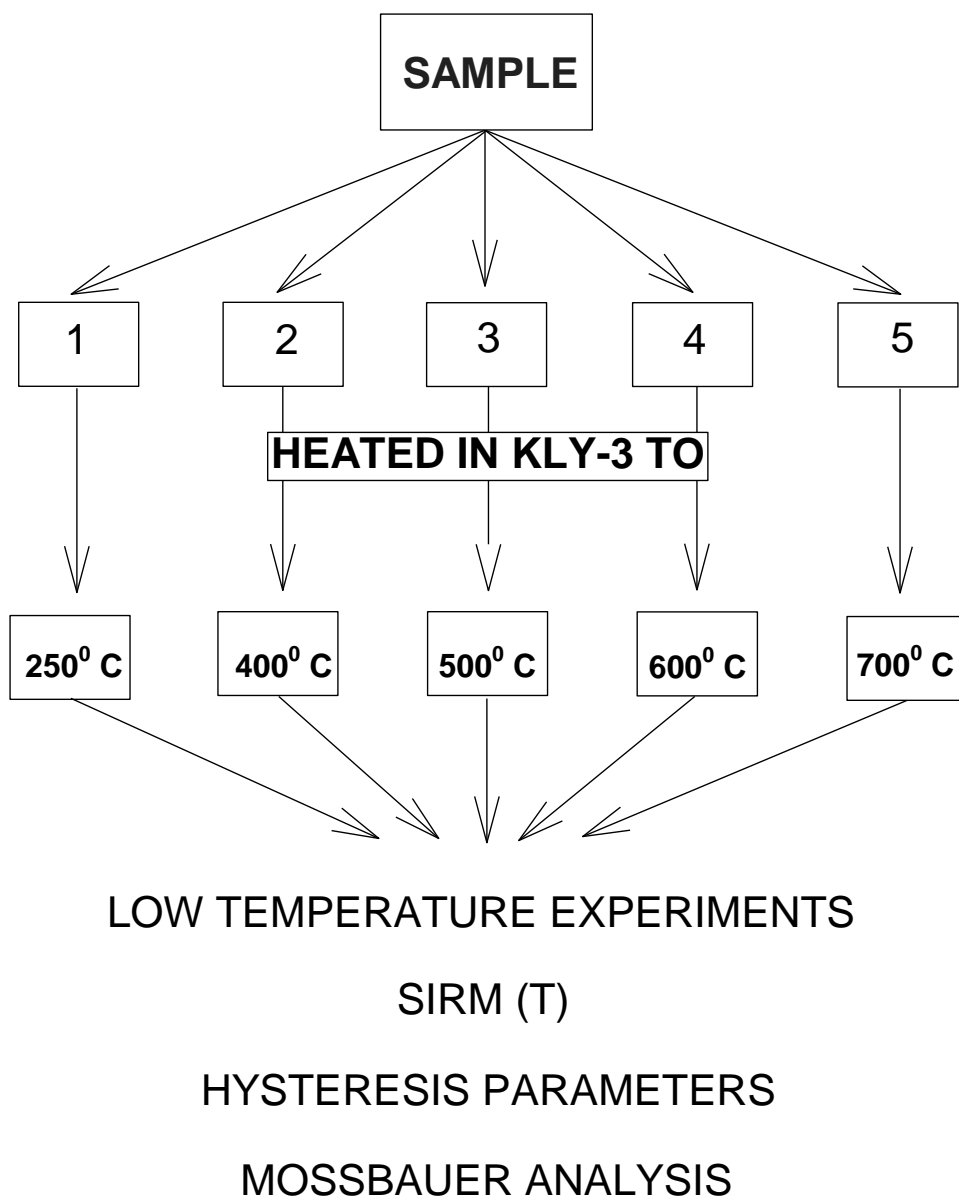


Fig. 3.

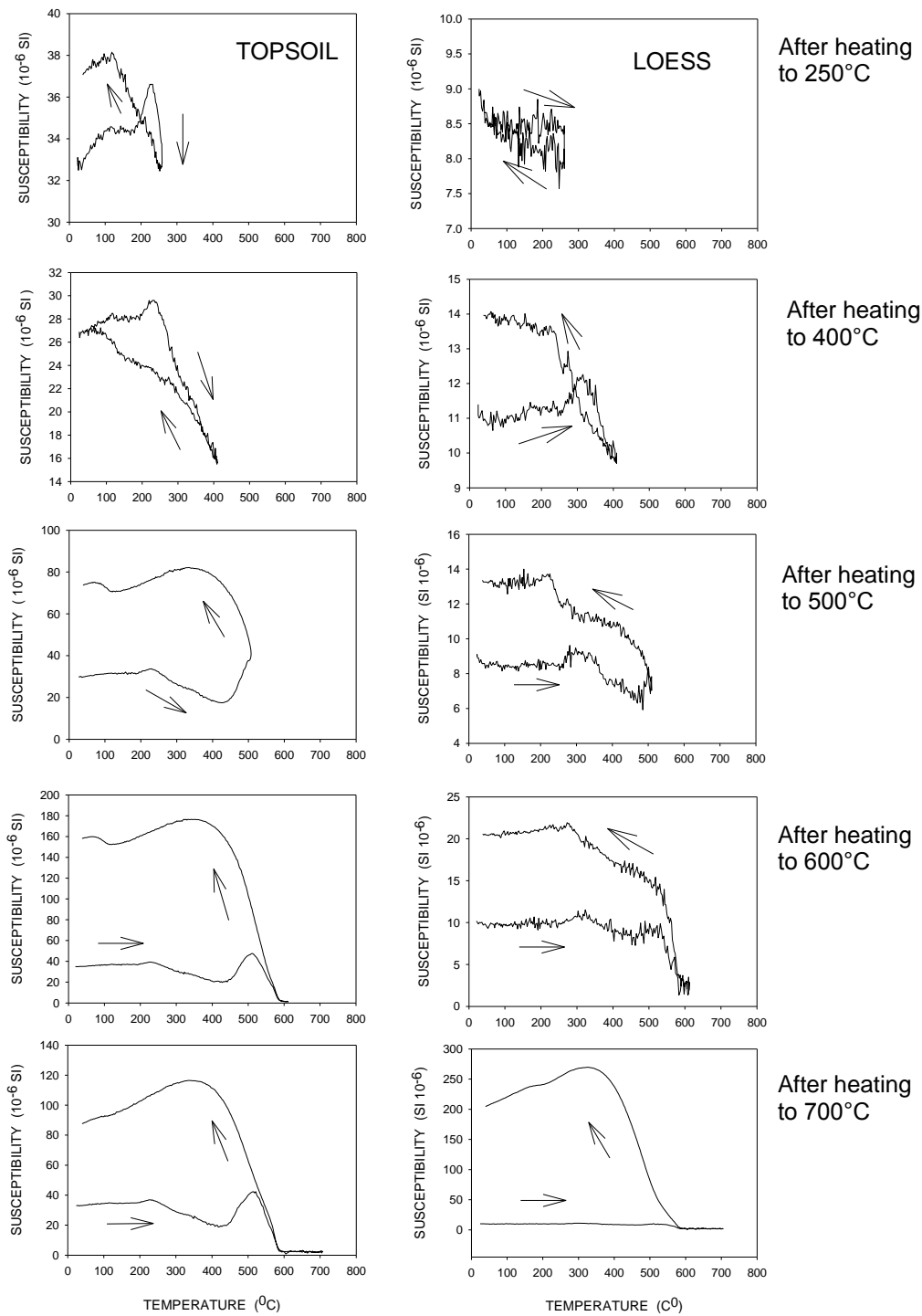


Fig. 4.

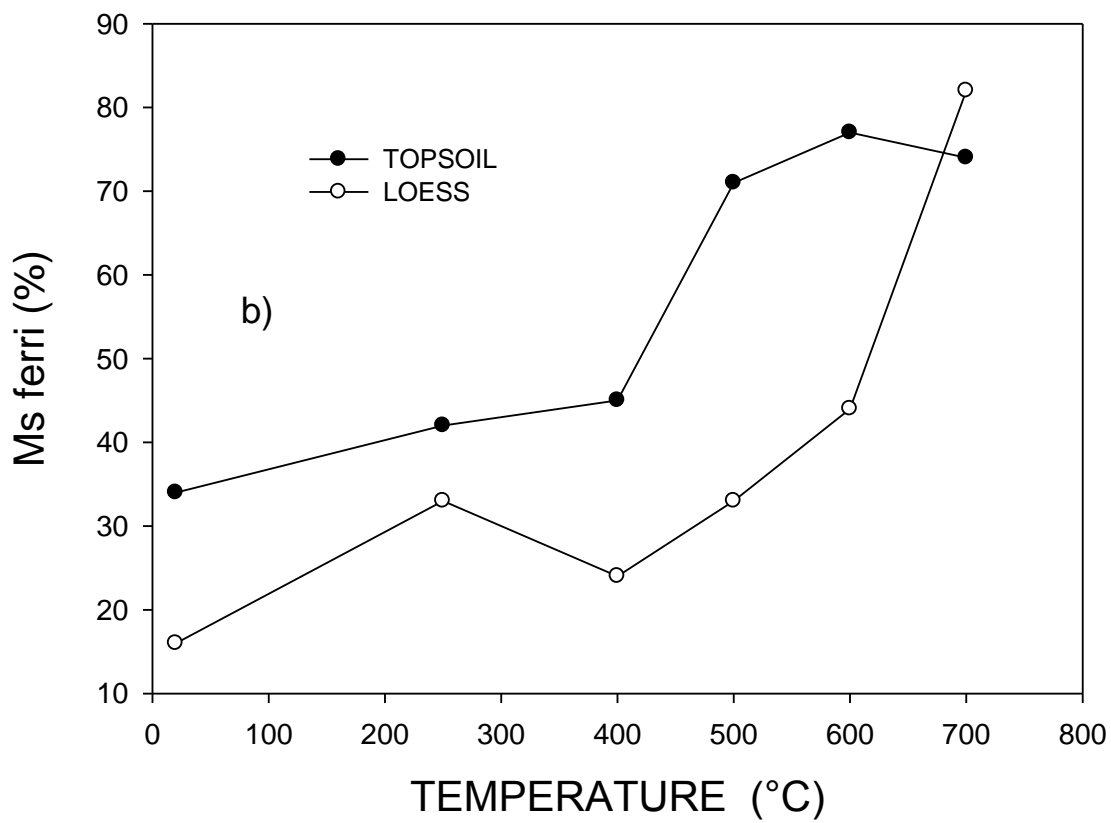
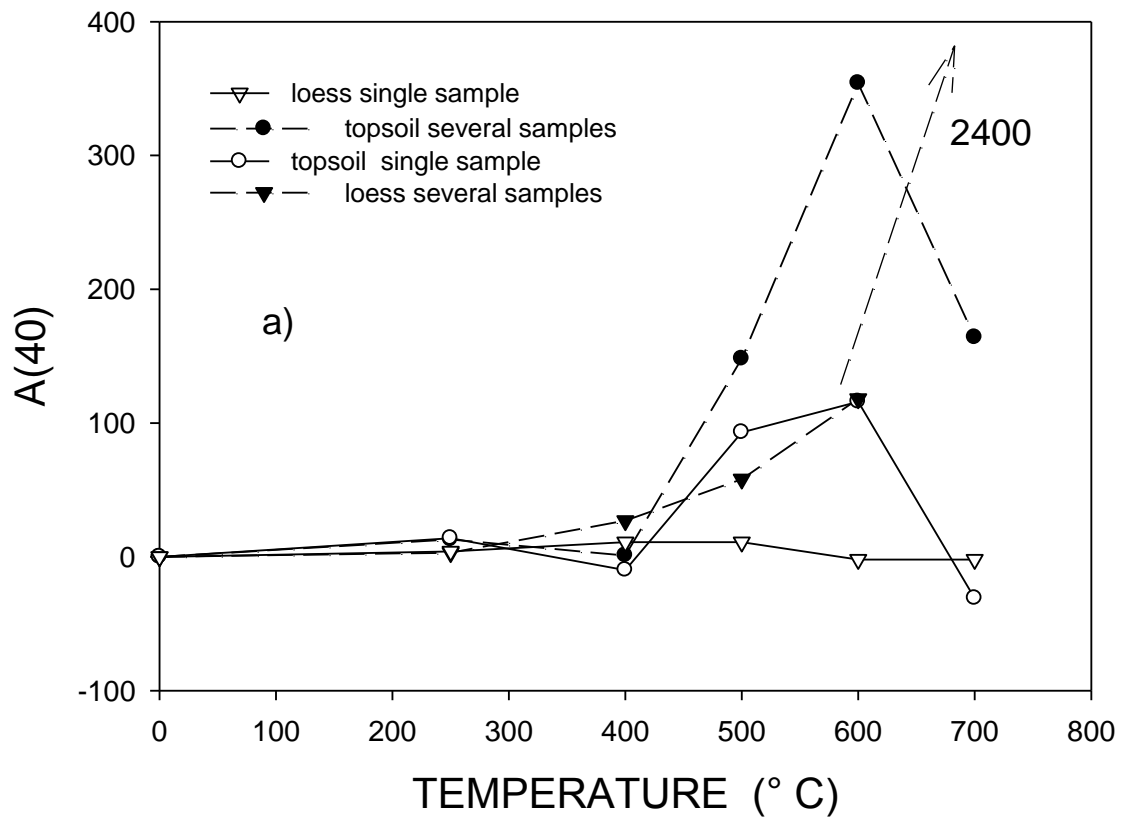


Fig. 5

Fig. 5.

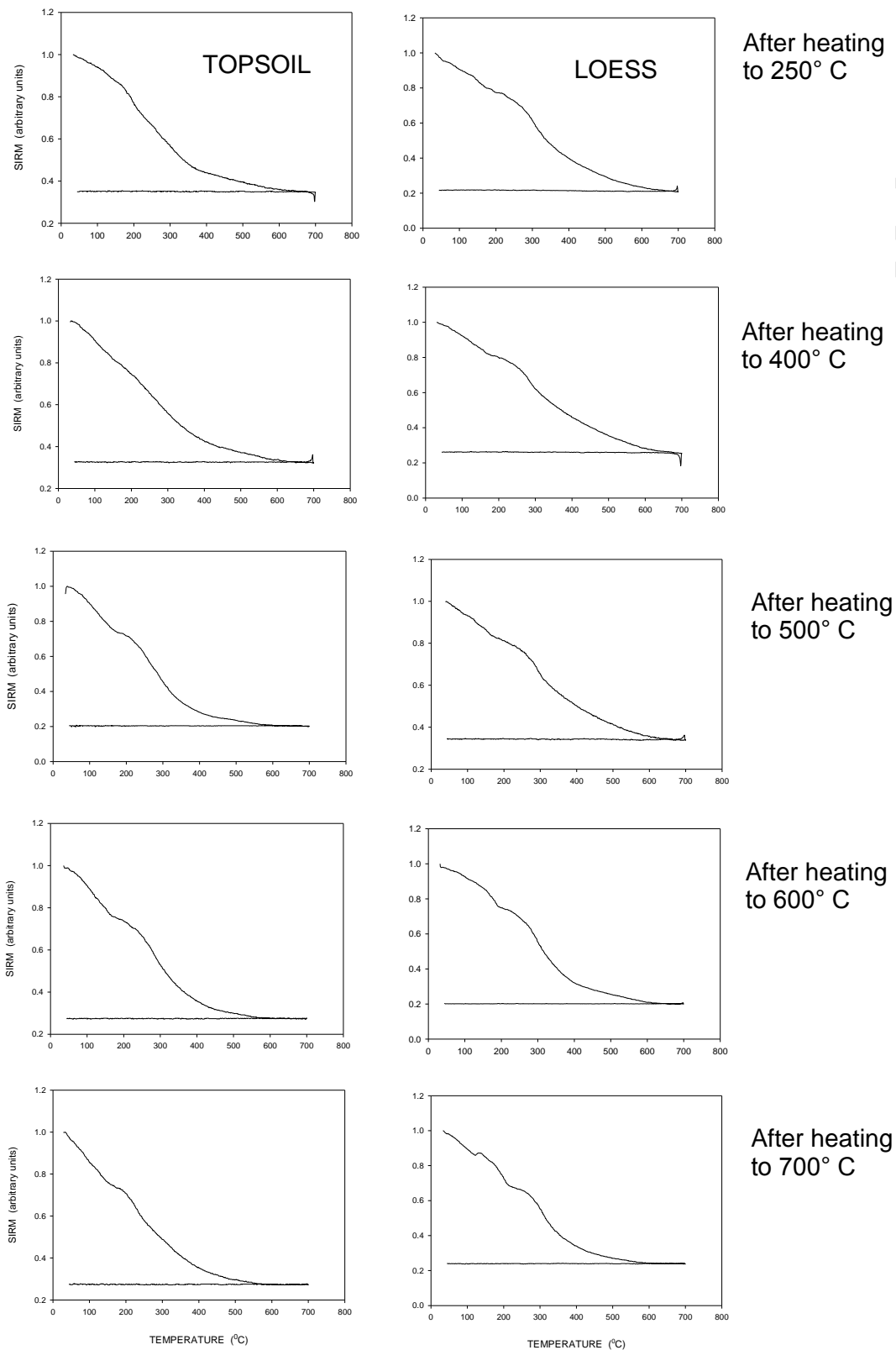


Fig. 6.

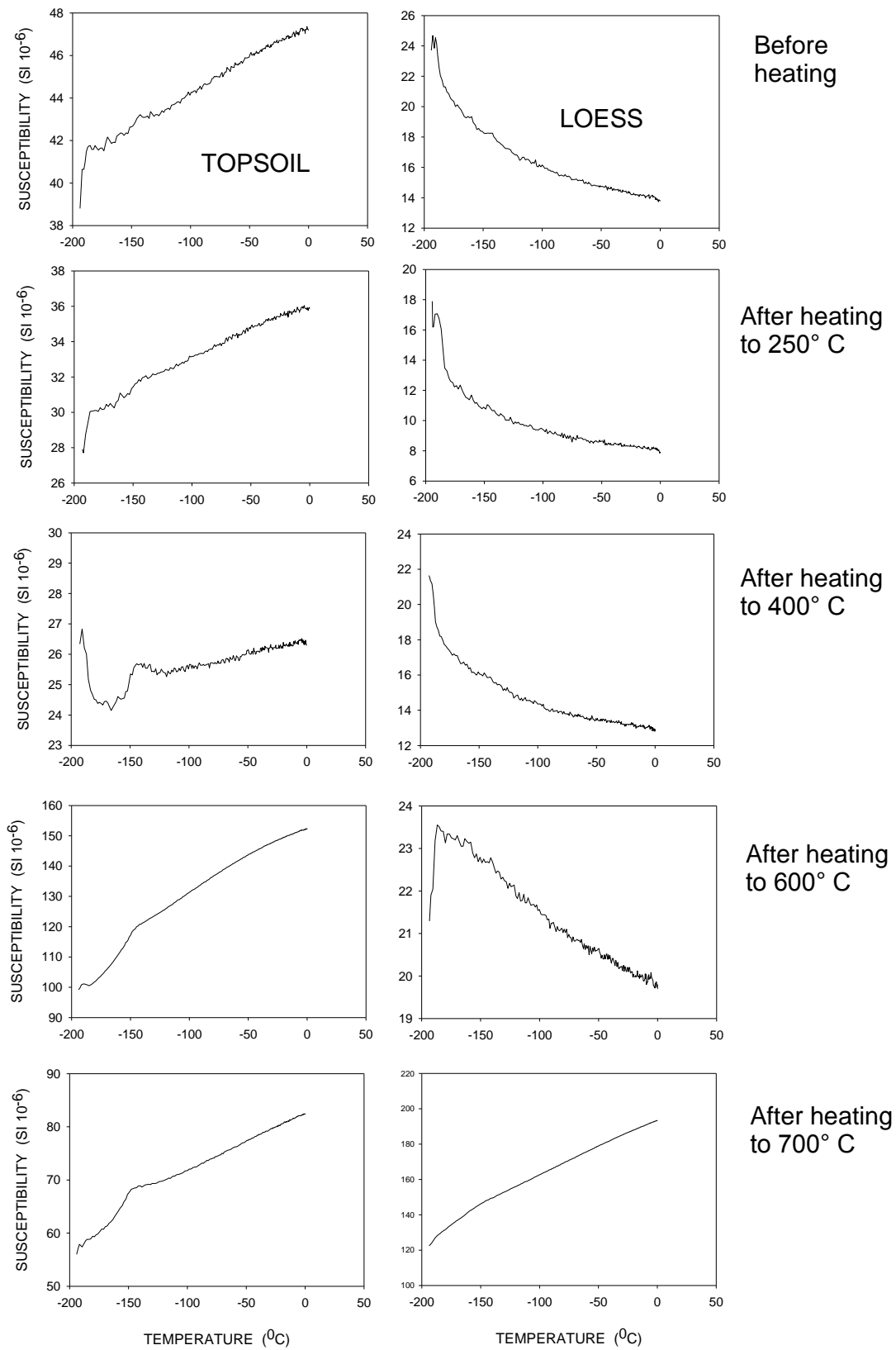


Fig. 7.

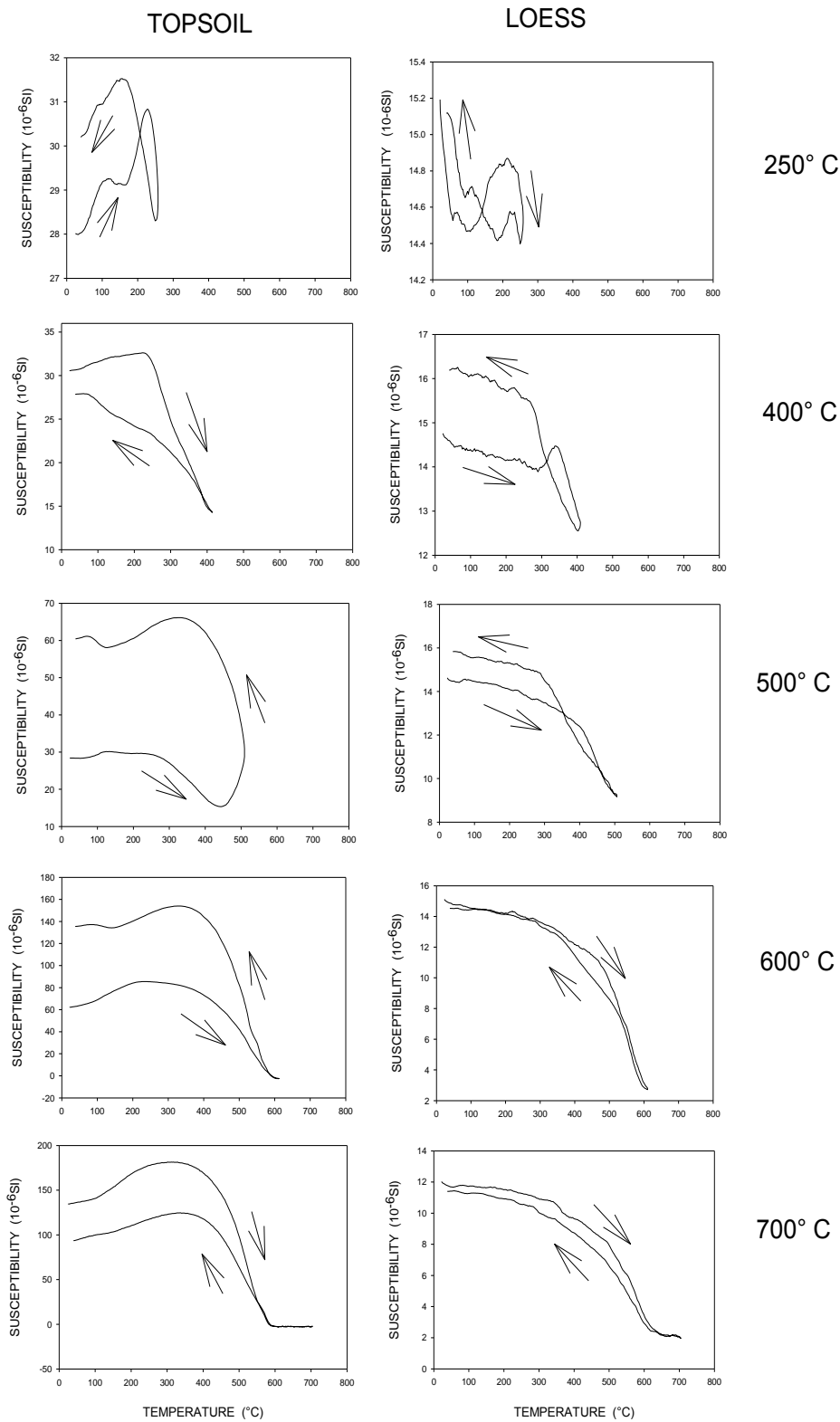


Fig. 8



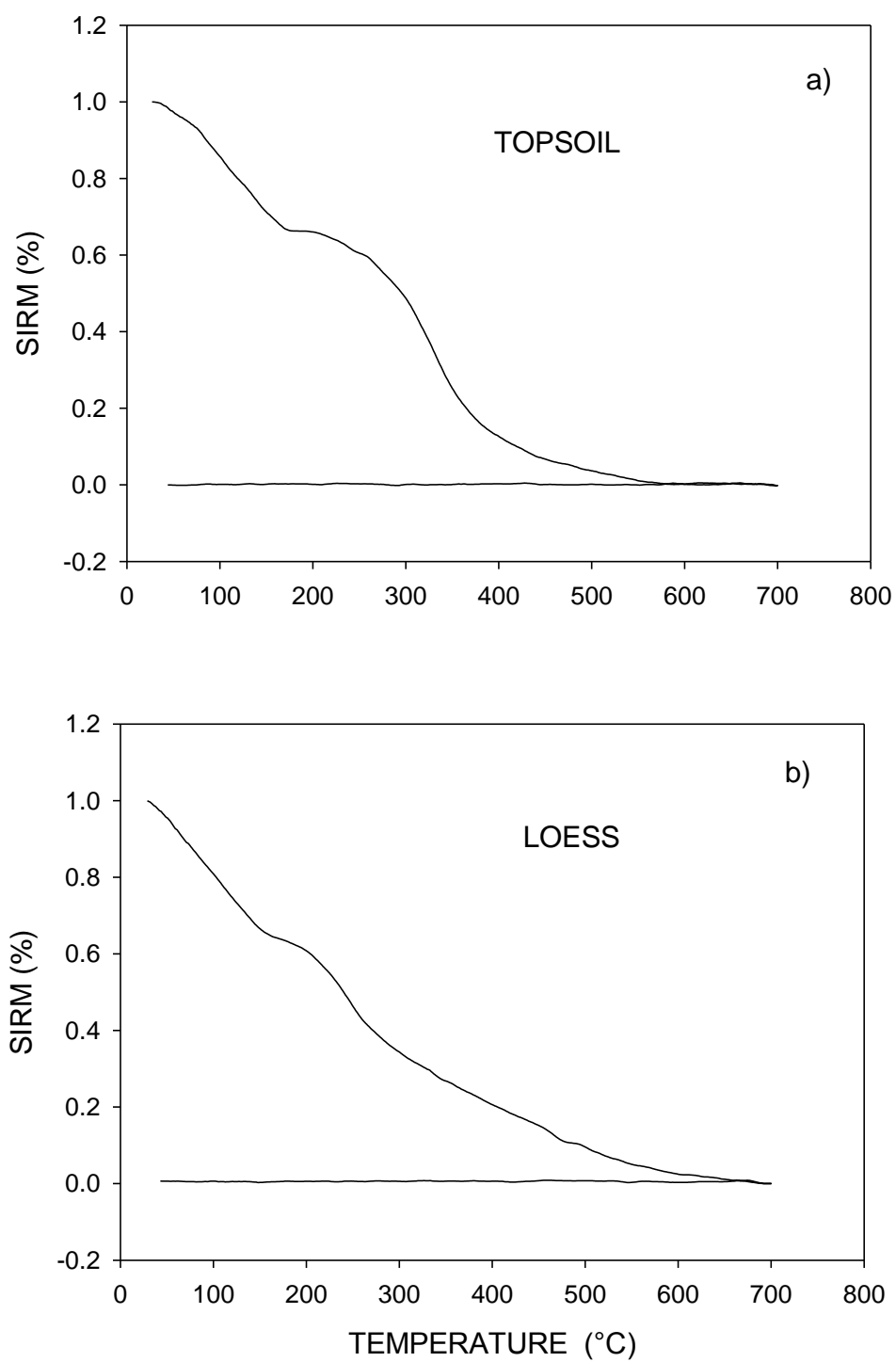


Fig. 9

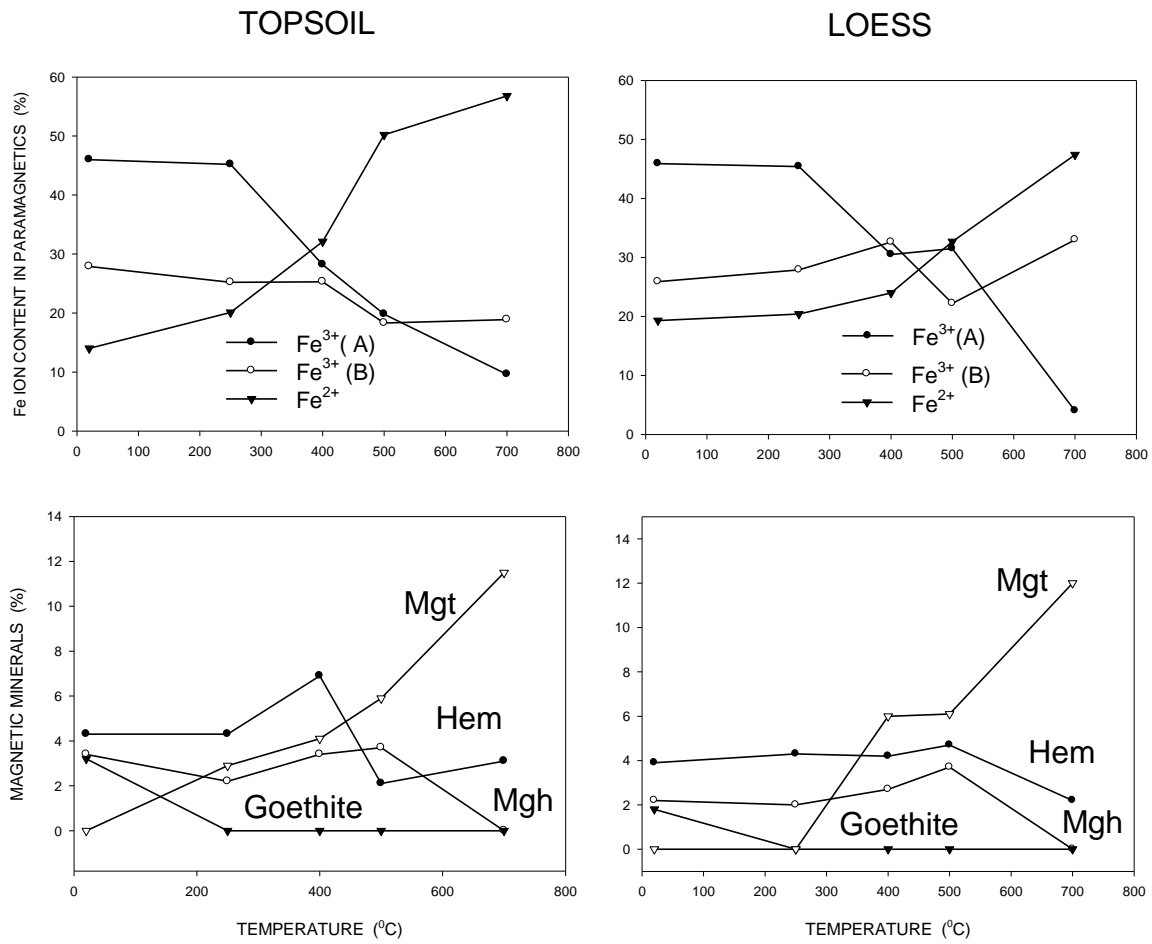


Fig. 10.

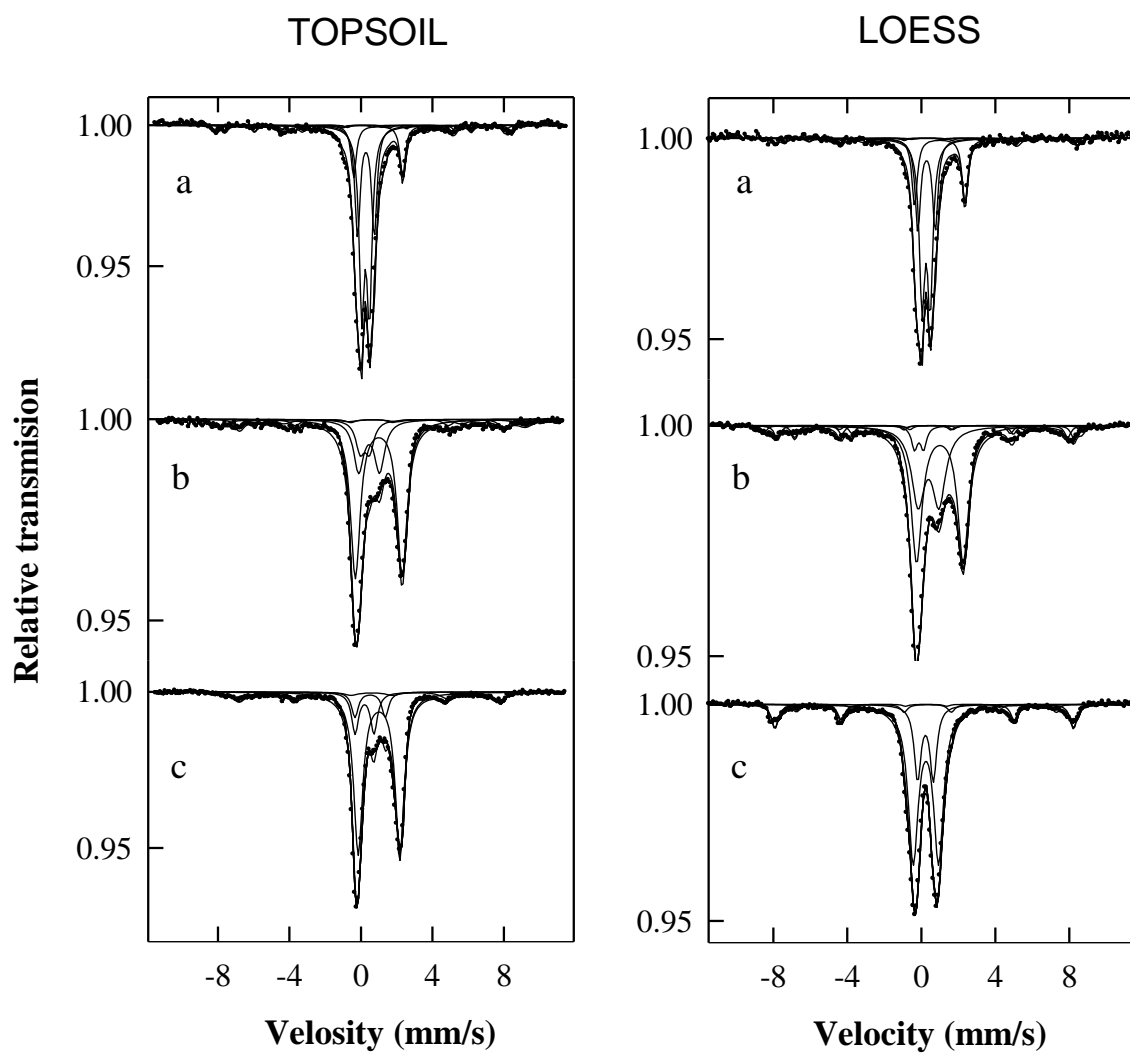


Fig. 11

Table 1. Chemical analysis of topsoil and loess.

Sample	pH	Humus (%)	Fe <sub>total</sub> (%)	Fe <sub>d</sub> (%)	Fe <sub>o</sub> (%)	Fe <sub>d</sub> /Fe <sub>total</sub>	Fe <sub>o</sub> /Fe <sub>d</sub>
Topsoil	7.59	6.87	3.33	0.657	0.095	0.197	0.145
Loess	9.04	0.55	2.74	0.530	0.035	0.193	0.066

Fe<sub>total</sub> – total content of iron determined by modified Lima-Jackson method (Cornell & Schwertmann 2003); Fe<sub>d</sub> - iron extracted with the sodium dithionite, the CBD Mehra-Jackson method (Mehra & Jackson 1960); Fe<sub>o</sub> - iron extracted with the acid NH<sub>4</sub> –oxalate, the AAO Tamm method (Mckeague & Day 1966). Fe<sub>d</sub> content has become a standard tool for determination of free iron oxides. Fe<sub>o</sub> content approximates amorphous or poorly crystalline iron oxides, mainly ferrihydrite. The ratio of Fe<sub>d</sub>/Fe<sub>total</sub> approximates the degree of transformation of original Fe-bearing minerals to pedogenic oxides (Cornell & Schwertmann 2003). The decreasing of the Fe<sub>o</sub>/Fe<sub>d</sub> ratio approximates the transformation of ferrihydrite to better crystalline oxides. Both ratios serve as indicators of the maturity of a soil.

Table 2. Changes of hysteresis parameters after heating.

T (°C)	RT	250	400	500	600	700	700/RT
<b>Topsoil</b>							
Ms (mAm <sup>2</sup> /kg)	37.2	43.3	51.9	204.3	380.0	316.6	8.5
Mr (mAm <sup>2</sup> /kg)	6.2	5.8	7.4	46.3	81.2	79.1	12.8
Hc (mT)	8.6	7.7	8.8	15.7	15.4	22.5	2.6
Hcr (mT)	28.4	27.2	31.5	35.4	38.3	50.6	1.8
Mr/Ms	0.17	0.13	0.14	0.23	0.21	0.25	
Hcr/Hc	3.3	3.5	3.6	2.25	2.5	2.25	
<b>Loess</b>							
Ms (mAm <sup>2</sup> /kg)	12.4	17.4	18.0	23.9	45.3	365.7	29.5
Mr (mAm <sup>2</sup> /kg)	2.5	2.6	2.8	3.9	9.8	82.5	33.0
Hc (mT)	14.0	11.1	10.8	11.0	16.5	12.6	0.9
Hcr (mT)	46.6	35.4	36.8	32.1	38.9	33.7	0.7
Mr/Ms	0.2	0.15	0.15	0.16	0.22	0.22	
Hcr/Hc	3.3	3.2	3.4	2.9	2.4	2.7	
<b>Topsoil (TS) /Loess (L)</b>							
Ms(TS)/Ms(L)	2.5	2.2	2.6	11.8	8.3	0.96	
Mr(TS)/Mr(L)	3.0	2.5	2.9	8.6	8.4	0.87	
Hc(TS)/Hc(L)	0.61	0.69	0.81	1.42	0.93	1.78	
Hcr(TS)/Hcr(L)	0.61	0.77	0.86	1.1	0.98	1.5	

T – heating temperature; RT – room temperature; TS – topsoil; L – loess.  
700/RT ratio of respective hysteresis parameter measured for fresh sample and sample heated to 700 °C.

Table 3. Relative area (%) of iron cations and magnetic minerals obtained by the Mössbauer analysis performed at room temperature for samples heated to different temperatures during susceptibility measurements.

T °C	Fe <sup>3+</sup> (A)	Fe <sup>3+</sup> (B)	Fe <sup>2+</sup>	$\alpha$ -Fe <sub>2</sub> O <sub>3</sub>	$\gamma$ -Fe <sub>2</sub> O <sub>3</sub>	$\alpha$ -FeOOH	Fe <sub>3</sub> O <sub>4</sub>
<b>Topsoil</b>							
RT	46	28	14	4	3	3	-
250	45	25	20	4	2	-	3
400	28	25	32	7	3	-	4
500	20	18	50	2	4	-	6
700	10	19	57	3	-	-	11
<b>Loess</b>							
RT	46	26	19	4	2	2	-
250	45	28	20	4	2	-	-
400	30	33	24	4	3	-	6
500	31	22	33	5	4	-	6
700	4	33	47	2	-	-	12

T – heating temperature; RT – room temperature.

Table 4. Mössbauer parameters for topsoil samples: fresh and heated in different way.

Component	Mössbauer hf parameters	Fresh sample	heated to 700°C	multi-heated up to 700°C
Fe <sup>3+</sup> minerals (A)	$\delta$ [mm/s]	0.36	0.32	0.45
	$\Delta$ [mm/s]	0.42	0.52	0.89
	RA[%]	46	10	16
Fe <sup>3+</sup> minerals (B)	$\delta$ [mm/s]	0.38	0.56	0.85
	$\Delta$ [mm/s]	0.93	1.27	1.64
	RA[%]	28	19	10
Fe <sup>2+</sup> silicate	$\delta$ [mm/s]	1.10	1.10	1.10
	$\Delta$ [mm/s]	2.73	2.62	2.43
	RA[%]	14	57	61
$\alpha$ - Fe <sub>2</sub> O <sub>3</sub>	$\delta$ [mm/s]	0.33	0.42	-
	H <sub>hf</sub> [T]	51.1	0.50	-
	RA[%]	4	3	-
$\gamma$ - Fe <sub>2</sub> O <sub>3</sub>	$\delta$ [mm/s]	0.28	-	-
	H <sub>hf</sub> [T]	48.6	-	-
	RA[%]	3	-	-
Fe <sub>3</sub> O <sub>4</sub> (Fe <sup>3+</sup> )	$\delta$ [mm/s]	-	0.74	-
	H <sub>hf</sub> [T]	-	53.1	-
	RA[%]	-	5	-
Fe <sub>3</sub> O <sub>4</sub> (Fe <sup>3+</sup> Fe <sup>2+</sup> )	$\delta$ [mm/s]	-	0.79	0.57
	H <sub>hf</sub> [T]	-	45.9	45.1
	RA[%]	-	6	13
$\alpha$ - FeOOH	$\delta$ [mm/s]	0.63	-	-
	H <sub>hf</sub> [T]	36.8	-	-
	RA[%]	3	-	-

$\delta$  – isomer shift;  $\Delta$  – quadrupole splitting, H<sub>hf</sub> – magnetic hyperfine field  
RA – relative area

Table 5. Mössbauer parameters for loess samples: fresh and heated in different way.

Component	Mössbauer hf parameters	Fresh sample	heated to 700°C	multi-heated up to 700°C
Fe <sup>3+</sup> minerals (A)	$\delta$ [mm/s]	0.36	0.32	0.33
	$\Delta$ [mm/s]	0.44	0.49	0.85
	RA[%]	46	4	20
Fe <sup>3+</sup> minerals (B)	$\delta$ [mm/s]	0.38	0.49	0.36
	$\Delta$ [mm/s]	0.95	1.13	1.37
	RA[%]	26	33	63
Fe <sup>2+</sup> silicate	$\delta$ [mm/s]	1.10	1.10	-
	$\Delta$ [mm/s]	2.72	2.52	-
	RA[%]	19	47	-
$\alpha$ - Fe <sub>2</sub> O <sub>3</sub>	$\delta$ [mm/s]	0.43	0.42	0.36
	H <sub>hf</sub> [T]	50.8	53.2	50.1
	RA[%]	4	2	13
$\gamma$ - Fe <sub>2</sub> O <sub>3</sub>	$\delta$ [mm/s]	0.28	-	0.37
	H <sub>hf</sub> [T]	48.6	-	48.4
	RA[%]	2	-	3
Fe <sub>3</sub> O <sub>4</sub> (Fe <sup>3+</sup> )	$\delta$ [mm/s]	-	0.38	-
	H <sub>hf</sub> [T]	-	49.8	-
	RA[%]	-	5	-
Fe <sub>3</sub> O <sub>4</sub> (Fe <sup>3+</sup> Fe <sup>2+</sup> )	$\delta$ [mm/s]	-	0.64	-
	H <sub>hf</sub> [T]	-	45.8	-
	RA[%]	-	7	-
$\alpha$ -FeOOH	$\delta$ [mm/s]	0.27	-	-
	H <sub>hf</sub> [T]	38.4	-	-
	RA[%]	2	-	-

Notation as in Table 3.